Assessment of an improved Random Flow Generation method to predict unsteady wind pressures on an isolated building using Large-Eddy Simulation

Romain Guichard

Assessment of an improved Random Flow Generation method to predict unsteady wind pressures on an isolated building using Large-Eddy Simulation

Romain GUICHARD*

*Institut National de Recherche et de Sécurité, Vandœuvre-lès-Nancy, F-54500, France.

romain.guichard@inrs.fr

Abstract

A wide variety of improved or modified Random Flow Generation (RFG) methods have recently been proposed for simulating the Atmospheric Boundary Layer (ABL) in a Large-Eddy Simulation (LES) framework. A distinct advantage of RFG methods over precursor-successor methods is the significant savings that can be made in terms of setup and computational costs. A review of the literature indicates that RFG methods are mostly evaluated in terms of velocity statistics and spectra. However, many applications in computational wind engineering ultimately aim to simulate the wind loads acting on a building. It would therefore be useful to evaluate the real capabilities of RFG methods for predicting unsteady wind pressures acting on various shapes of building. In this paper, one of the available RFG methods based on a summation of Fourier harmonic functions is assessed for various shapes of isolated building (a full-scale cube, a wind-tunnel cube, a high-rise building and a low-rise building) in terms of pressure statistics and spectra. Comparisons between measurements and simulations show that the RFG method tested here could be particularly relevant for industrial applications, provided that the inlet turbulence intensity profile is adapted.

Keywords

Large-Eddy Simulation, Random Flow Generation, wind pressure, building.

1. Introduction

The ability to predict the flow around a building is necessary in a wide variety of applications in wind engineering, including pollutant dispersion in urban areas, wind resistance of buildings and wall cladding, and dynamic containment of airborne pollutants. To assess the effectiveness of dynamic containment when subjected to wind, as encountered in asbestos removal worksites (Papadopoulos et al., 2018) and nuclear plants (Le Roux et al., 2013), it is

necessary to know the unsteady differential pressure between the indoor and outdoor environments, together with the local wind characteristics.

The first step in identifying and subsequently preventing containment breaches is thus to simulate the airflow around the building in question. Large-Eddy Simulation (LES) is one of the most widely used tools for simulation of the Atmospheric Boundary Layer (ABL), being increasingly adopted due to recent increases in computational power and the growth of unsteady problems investigation.

The influence of the majority of simulation parameters used in computational wind engineering is either negligible or can be controlled such as for ground roughness, the subgrid-scale model, the domain size, the near-wall treatment, and sensitivities to mesh and timestep (Blocken, 2015, Franke et al., 2010, Guichard, 2017, Tominaga et al., 2008). However, turbulent inflow conditions are known to have a strong influence on numerical results. Richards and Norris (2015) demonstrated that in the absence of similar turbulence intensity profiles in the simulation and experiment, it was impossible to achieve accurate wind pressures at the building.

In order to produce realistic velocity and turbulence inflow fields, various techniques based on either a precursor domain or a synthetic turbulence generator have been proposed and discussed in the literature. Methods based on a precursor domain, with or without recycling, generally involve a higher computational cost due to the use of explicit roughness elements or the iterative adjustment of simulation parameters to obtain the targeted ABL. For these reasons, synthetic turbulence generators that ensure divergence-free inflow fields, like for example the RFG (Kraichnan, 1970, Smirnov et al., 2001), the efficient generation method for street-scale flows (Xie and Castro, 2008), the DSRFG (Huang et al, 2010), the MDSRFG (Castro and Paz, 2013), the improved SEM (Poletto et al., 2013), the CDRFG (Aboshosha et al., 2015) and the NSRFG (Yu et al., 2018) are preferred for practical applications. However, these methods all suffer from a significant decrease in turbulence intensity between the inlet and the building location as the inflow provided is not consistent with the system of equations that is solved in the domain, as explained in Lamberti et al. (2018) and observed by Vasaturo et al. (2018). Although it is then impossible to achieve streamwise homogeneity, Vasaturo et al. (2018) show that the Gaussian velocity spectra produced by the RFG at the inlet rapidly evolve along the domain towards the same shape as those obtained with recycling and Vortex methods, but with a much lower power spectral density. Moreover, previous studies have shown that if the issue of the decrease in turbulence intensity along the computational domain

can be overcome, then realistic wind pressure coefficients can be achieved (Yan and Li, 2015).

The objective of this paper is to evaluate an efficient way for obtaining targeted velocity and turbulence intensity profiles at the building location. Computational and experimental wind pressure coefficients are compared for different shapes of isolated building. The approach was inspired by wind tunnel tests that aim to obtain targeted profiles at the future building location and not necessarily to achieve full streamwise homogeneity, as shown by the partial covering of the wind-tunnel ground by roughness elements. In the framework of practical applications in wind engineering, the RFG method of Smirnov et al. (2001) has been retained here as it does not require any additional developments to the widely used ANSYS Fluent code, and because the code verification has already been done. This is a criterion of choice for engineers as it means that the method can be applied immediately, though it must first be clearly validated for each field of industrial applications. The RFG method, available under the name Spectral Synthesizer, produces a continuous flow field as a superposition of one hundred Fourier harmonic functions. It involves scaling and orthogonal transformation operations to guarantee a flow field that is divergence-free for homogeneous turbulence and nearly divergence-free for inhomogeneous turbulence.

The methodology, simulation setup, and reference experiments used to fulfil the objective of this paper are described in the next sections and are followed by a discussion of the results.

2. Methodology

The procedure that was eventually selected to apply the RFG to computational wind engineering cases in this paper is close to that denoted “improved RFG” in Yan and Li (2015). It consists of three steps, as illustrated in Figure 1:

Step 1 – Generation of the targeted inflow (from experimental or theoretical data) using RFG in an empty domain,

Step 2 – Explicit adjustment of inlet boundary conditions using Eq. (1) to achieve targeted profiles at the future building location,

Step 3 – Running the final computation using RFG in the domain with the building.

The procedure differs from the “improved RFG” method of Yan and Li (2015) in that only one adjustment is required and the method does not require successive trial-and-error iterations to obtain the targeted profile. It is assumed here that the mean velocity profile is homogeneous, that the length scale remains unchanged and that the turbulence intensity profile is adapted according to:

$$I_{adapted}(z) = I_{target}(z) + \Delta x\left(\frac{I_{target}(z) - I_{building}(z)}{\Delta x}\right) = 2I_{target}(z) - I_{building}(z), \quad (1)$$

where z is the vertical coordinate, Δx is the streamwise distance between the inlet and the building, $I_{building}$ is the turbulence intensity first obtained at the future building location in the empty domain, I_{target} is the targeted turbulence intensity and $I_{adapted}$ is the turbulence intensity to be used in the final computation. When verification is required, it is still possible to ensure that I_{target} is accurate at the building location in an empty domain. In this paper, the verification is presented in the Results and Discussion sections.

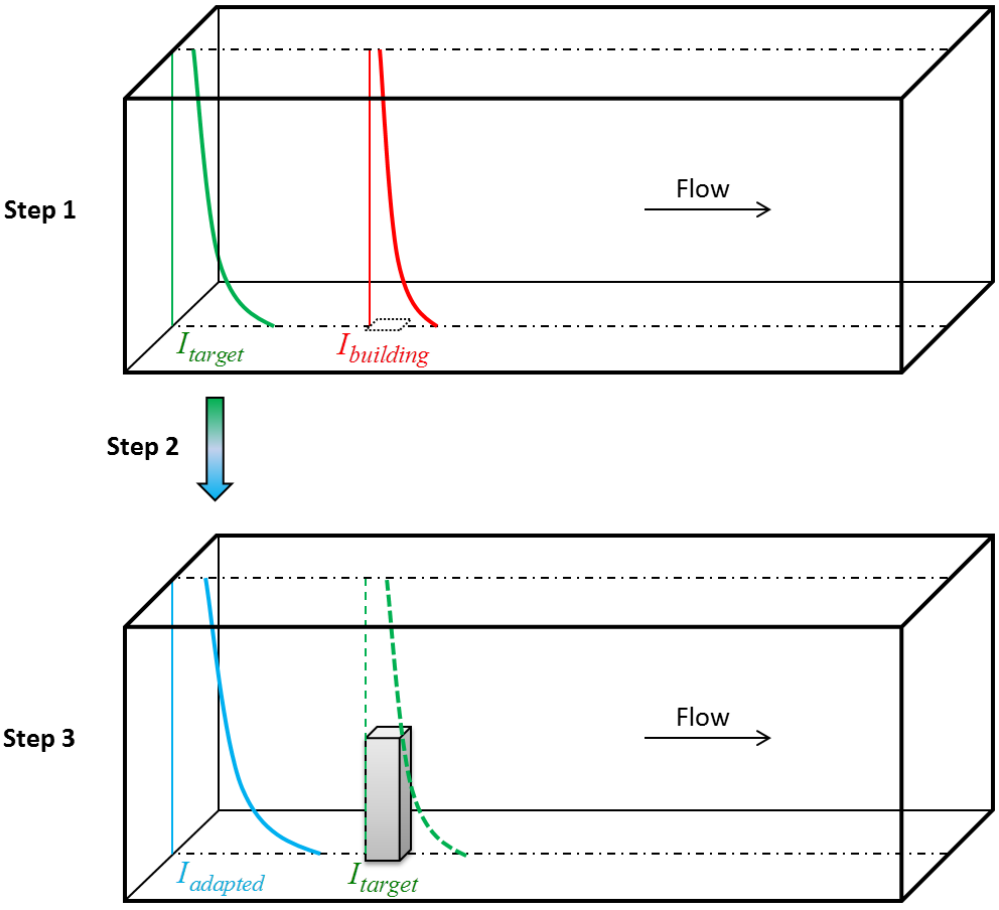

Figure 1 Strategy applied to obtain the targeted turbulence intensity profile at the building location using the RFG method

3. Simulation setup

The simulation setup is as far as possible kept unchanged or parameterized. Only the domain size, which is a function of building height, and the inlet profiles are updated for each study case.

3.1 Computational domain and grid

The computational domain is built by strictly following the guidelines of Franke et al. (2010), hence the inlet, lateral and upper boundaries are 5H away from the building and the outlet boundary is 15H behind the building (where H is the height of the building).

Use of the cut-cell meshing technique, as verified in Iousef et al. (2017) in a close framework, allows a very good mesh quality to be obtained, and it is also easy to manage. This technique also limits the number of parameters needed to describe the mesh if one wants to exactly reproduce the same mesh. A grid sensitivity study has led to application of the following cell sizes:

- at building faces, the length of the shortest building edge divided by 15,
- at the ground: twice the cell size set at building faces,
- elsewhere: twice the cell size set at the ground.

In addition, an inflation growth factor of 1.1 is applied, which allows the number of uniform layers before switching from one cell size to another to be controlled. These meshing settings result in a rather coarse mesh of one million cells and an average y^+ of 300. An example of such a mesh for a high-rise building is provided in Figure 2.

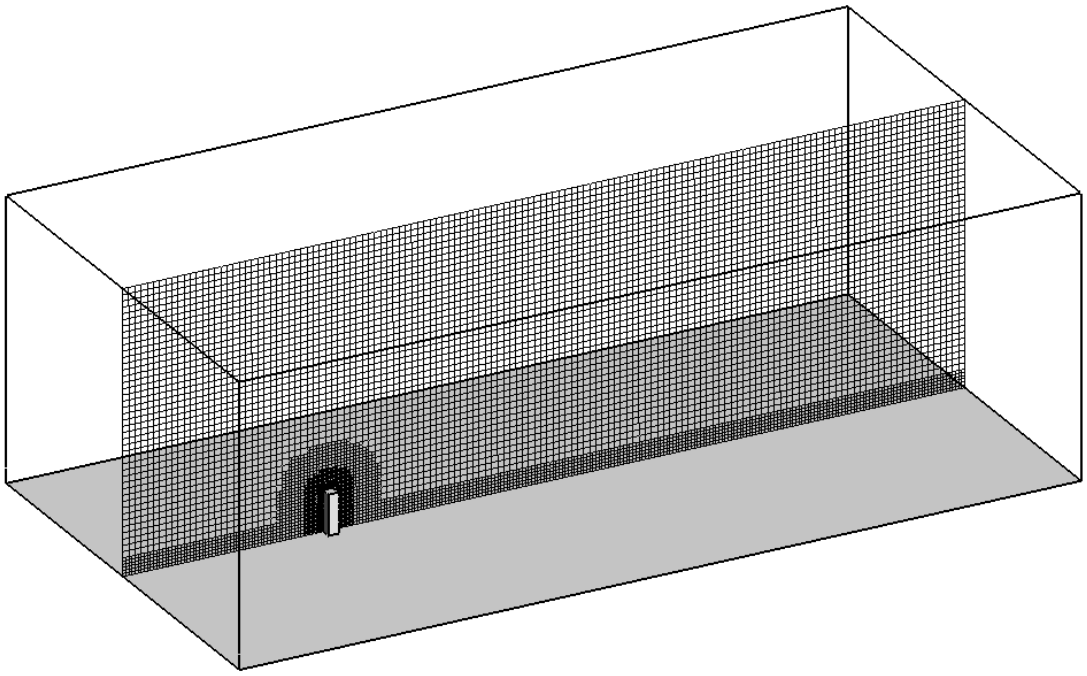

Figure 2 Example of a mesh in a center cut plane, generated with the cut-cell technique for a high-rise building

3.2 Boundary conditions

Symmetry conditions are applied to upper and lateral boundaries. This implies zero normal velocity and zero gradients for all variables. The inlet is a velocity-inlet and the outlet is a pressure-outlet boundary condition. Both ground and building are smooth walls as various sensitivity studies have shown that ground roughness has only a weak influence on the performance on the performance of inflow methods (Köse and Dick, 2010; Vasaturo et al., 2018). The upstream ground roughness is taken into account through the aerodynamic roughness length in the inlet profiles.

The target profiles are best fits of the available experimental data, based on the wind profile log law (Oke, 1987):

$$U(z) = \frac{u_\tau}{\kappa} \log\left(\frac{z + z_0}{z_0}\right), \tag{2}$$

where U is the mean air velocity, $\kappa = 0.4$ is the von Kàrmàn constant, z_0 is the aerodynamic roughness length, and u_τ is the friction velocity defined by

$$u_\tau = \kappa \frac{U_H}{\log\left(\frac{H + z_0}{z_0}\right)}, \tag{3}$$

where H is the building reference height.

Depending on the experiments considered, a better fit can be achieved using the wind profile power law of Counihan (1975):

$$U(z) = U_H \left(\frac{z}{H} \right)^{\alpha}, \tag{4}$$

where α is the stability and roughness exponent.

As the turbulence intensity rather than the turbulence kinetic energy is often provided in experimental data, the turbulence kinetic energy profile can be computed as:

$$k(z) = \frac{3}{2}\left(U(z) I(z)\right)^2, \tag{5}$$

where I is the measured turbulence intensity, which is least-squares fitted using the following expression:

$$I(z) = I_u^{\infty} + \left(I_u^{g} - I_u^{\infty}\right)\exp(-az), \tag{6}$$

where I_u^{∞} is the bulk turbulence intensity parameter, I_u^{g} is the ground turbulence intensity parameter and a is the curvature parameter.

Finally, given that the turbulence length scale is not provided in reference experiments, the turbulence dissipation rate is set as:

$$\varepsilon(z) = \frac{u_\tau^3}{\kappa(z + z_0)}. \tag{7}$$

The quality of the representation of available experimental data by Eq. (2) to (7) will be verified in the Results and Discussion sections below.

3.3 Numerical settings

The CFD solver ANSYS Fluent 17.2 was used for all simulations. As the mesh is too coarse to resolve the laminar sub-layer, a wall function must be used. A law-of-the-wall was therefore applied to compute the wall shear stresses with the assumption that the centroid of the wall adjacent cell was in the logarithmic region of the boundary layer. This approach is called Standard Near-Wall Treatment. Because LES is based on the filtering of Navier-Stokes equations, a Sub-Grid Scale model must be used for that part of the turbulence spectrum that is not resolved. The Wall-Adapting Local Eddy-Viscosity (WALE) formulation proposed by Nicoud and Ducros (1999) was used here. In contrast with constant and dynamic Smagorinsky-Lilly models, a spatial operator is added to the eddy viscosity formulation to provide the expected wall asymptotic behavior.

Regarding the spatial discretization, a second-order scheme was chosen for pressure and a bounded-central-differencing scheme was chosen for momentum.

For the temporal discretization, a Non-Iterative Time Advancement (NITA) was set, along with a fractional-step pressure-velocity coupling. The corresponding algorithms are detailed in the ANSYS Fluent Theory Guide (2016). Fixed timesteps were deduced from RANS k-ε Realizable simulations to strictly respect the CFL condition in each cell. The LES initialization run was first conducted over a period of 6 flow-through times, and flow statistics were then computed over 30 flow-through times.

4. Reference experiments

4.1 The Silsoe cube full-scale experiment

The Silsoe cube experiment is one of the most well-documented full-scale investigations of wind velocities and pressures on a building found in the literature (Richards and Hoxey, 2012). It is crucial to include full-scale data for validation as reduced-scale models are not always able to reproduce every characteristic of real wind (Richards et al., 2007; Irtaza et al., 2013). Full-scale data therefore represents the experimental data that are the closest to final wind engineering applications. The building considered here is a 6 m cube, instrumented with pressure taps along vertical and horizontal centerlines, as shown in Figure 3.

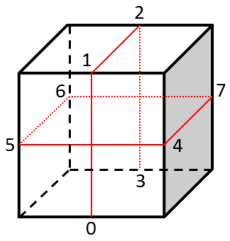

Figure 3 Centerlines along which pressure taps are distributed in the Silsoe cube experiment (the front face is windward)

The flat ground on which the cube is mounted is composed of grass, which leads to an aerodynamic roughness length z_0 of 0.01 m. The mean velocity is 6 $m.s^{-1}$ and the turbulence intensity is around 20 % at the height of the building. For this reference experiment, wind mean velocity and turbulence intensity profiles are provided, in addition to the mean, standard deviation, and minimum and maximum pressure coefficients. These parameters allow the

quality of both the inflow conditions and the pressure statistics acting on a building to be evaluated. The pressure coefficients C_p are defined by:

$$C_{p,\text{mean}} = \frac{p_{\text{mean}}}{q_{\text{mean}}},\ C_{p,\text{min}} = \frac{p_{\text{min}}}{q_{\text{max}}},\ C_{p,\text{max}} = \frac{p_{\text{max}}}{q_{\text{max}}},\ C_{p,\text{std}} = \frac{p_{\text{std}}}{q_{\text{std}}}, \quad (8)$$

where p is the static pressure on the building, q is the reference dynamic pressure and the subscripts 'mean', 'min', 'max' and 'std' are the mean, minimum, maximum and standard deviation values, respectively.

4.2 Tokyo Polytechnic University (TPU) wind-tunnel experiments

An assessment of a proposed approach is not complete if only one study case is considered. The Tokyo Polytechnic University (TPU) aerodynamic database was therefore exploited in addition to the Silsoe cube experiment.

A particular advantage of the extensive TPU database is that it provides time series of wind pressure coefficients. Of the various wind-tunnel experiments available in the database, three cases were retained here:

- a reduced-scale (1:400) cube of 0.1 m, to consolidate the full-scale case described in the previous section with a different approaching flow and a different scale. In this case the flow exponent was 0.25, the mean velocity was 7 $m.s^{-1}$ and the turbulence intensity was 23 % at building height. Tests were run over 32.768 s with a frequency of 1000 Hz.
- a reduced-scale (1:400) high-rise building with dimensions of 0.1 m (width) x 0.2 m (length) x 0.4 m (height), as this type of tall building is often highly exposed to wind. The flow exponent was 0.25, the mean velocity was 11 $m.s^{-1}$ and the turbulence intensity was 12 % at building height. Tests were run over 32.768 s with a frequency of 1000 Hz.
- a reduced-scale (1:400) low-rise building with dimensions of 0.16 m (width) x 0.4 m (length) x 0.08 m (height) in order to evaluate a common shape of industrial building. The flow exponent was 0.25, the mean velocity was 7 $m.s^{-1}$ and the turbulence intensity was 24 % at building height. Tests were run over 18 s with a frequency of 500 Hz.

It is important to note that in the TPU database, the pressure coefficients have a different definition to those of the Silsoe experiment:

$$C_{p,\text{mean}} = \frac{p_{\text{mean}}}{q_{\text{mean}}},\ C_{p,\text{min}} = \frac{p_{\text{min}}}{q_{\text{mean}}},\ C_{p,\text{max}} = \frac{p_{\text{max}}}{q_{\text{mean}}},\ C_{p,\text{std}} = \frac{p_{\text{std}}}{q_{\text{mean}}}. \quad (9)$$

For the sake of clarity, it is impossible to plot all experimental and numerical pressure coefficients for each face of each building. The results will therefore be compared in two

rings, as illustrated in Figure 4, along which the pressure taps were placed in the wind-tunnel experiments.

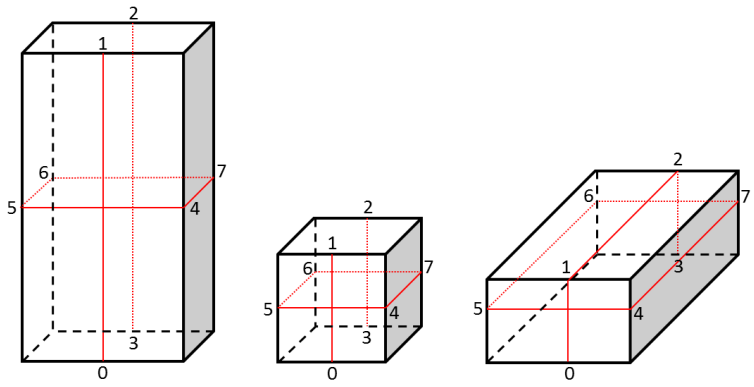

Figure 4 Lines along which pressure coefficients were processed in TPU experiments (front faces are windward)

5. Results and discussion

5.1 Verification of targeted mean velocity and turbulence intensity

The first step in the evaluation is to verify that the simulated profiles at the building location are consistent with the measured profiles when the strategy described in Figure 1 is applied using RFG as an inlet velocity fluctuations synthesizer. For each case considered, the targeted mean velocity profiles are reproduced in Figure 5 and the turbulence intensity profiles are presented in Figure 6. The indices u, v, w denote the streamwise, spanwise and vertical directions, respectively. Note that only the streamwise component of the turbulence intensity is provided for the TPU cases.

Figures 5 and 6 clearly show that the RFG method can produce velocity and turbulence intensity profiles that are very close to the targeted experimental data, after adjustment of the turbulence intensity. When the three components of turbulence intensity are available, the tested RFG is even able to reproduce the expected relationships between them (Counihan, 1975), namely $I_v = 0.75\ I_u$ and $I_w = 0.5\ I_u$ from the ground to building height. These simulated profiles are also much more accurate than those obtained in the wind-tunnel modeling of the Silsoe cube in Aukland (Richards et al., 2007). Figure 6 also shows that vertical profiles of turbulence intensity differ significantly from one wind-tunnel test to another, the turbulence intensity in Figure 6 varying from 25% at the ground to 2% at a height of 6H for the high-rise building, but ranging from 25% to 20% for the low-rise building, being almost flat.

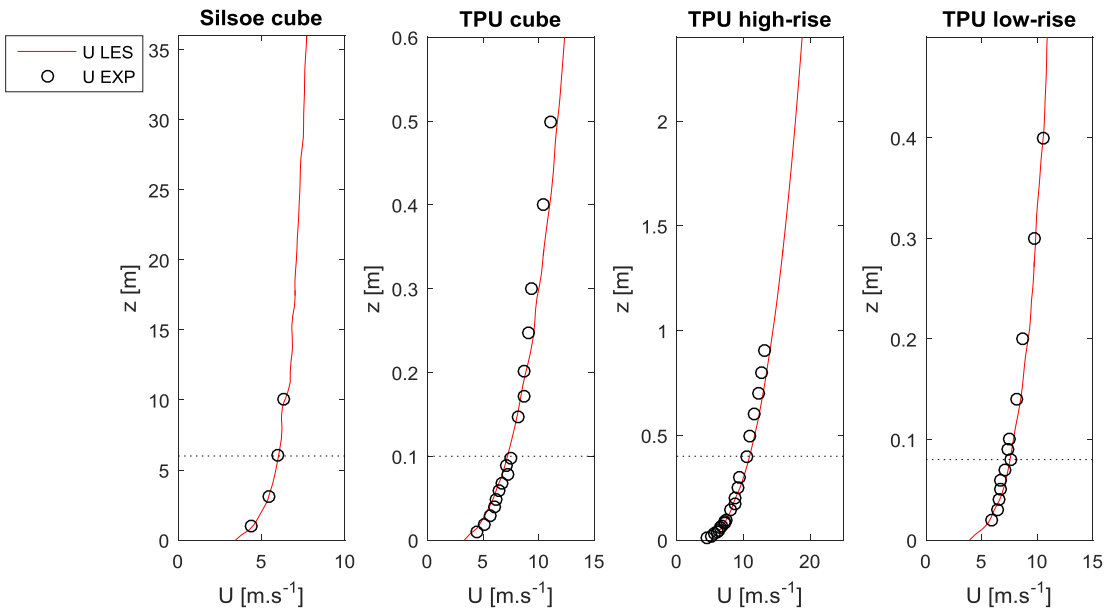

Figure 5 Comparison of simulated and measured vertical profiles of mean velocity at the building location

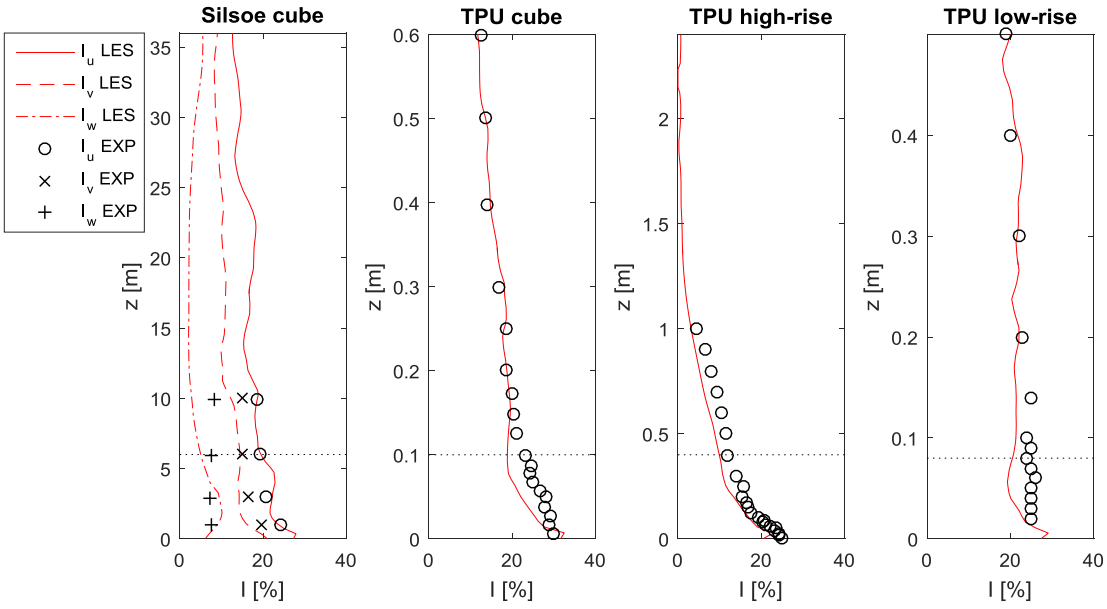

Figure 6 Comparison of simulated and measured vertical profiles of turbulence intensity at the building location

To further evaluate the flow characteristics at the building location, the streamwise velocity spectrum at building height is plotted in Figure 7, superimposed with the Gaussian spectrum produced by the RFG method at the inlet. The results highlight that the inlet spectrum evolves towards a more representative spectrum when approaching the building location, as

previously reported by Vasaturo et al. (2018). This means that the flow obtained at the building location might eventually be closer to the experimental flow than expected.

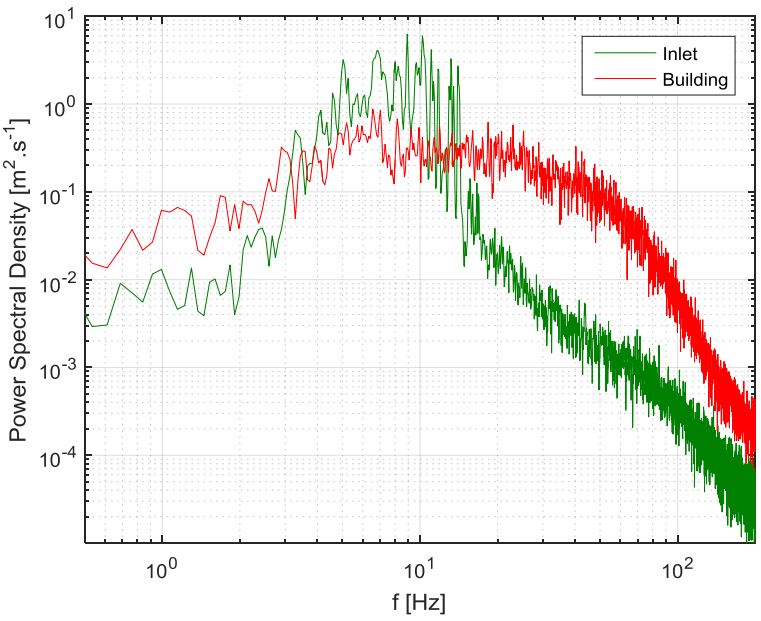

Figure 7 Velocity spectra at the building height in the TPU cube case, as simulated at the inlet and building locations

5.2 Pressure coefficients

The mean, minimum, maximum and standard deviation of pressure coefficients are presented in Figure 8. Results obtained by Large-Eddy Simulation are plotted using lines and are denoted by LES in the legend. Experimental data are plotted with symbols and denoted by EXP. The normalized abscissa corresponds to the numbers depicted in Figures 3 and 4. Overall, the computed pressure coefficients are in good agreement with experimental data for the buildings considered. The major deviation is observed for peak values, which are known to be more difficult to accurately predict and will be discussed below. For the Silsoe cube case however, the simulations provide a better prediction of standard deviation and peak pressure coefficients than others in the literature (Richards and Norris, 2015). This is mainly due to the fact that the flow generated at the building location in the present paper is much closer to the full-scale experiment than in previous studies. One of the implications of this for current industrial applications is that the best results can be obtained if the focus is more on flow characteristics at the building location than on the streamwise flow homogeneity, though such a choice of emphasis would not be relevant in the framework of fundamental research. Another observation is that the discrepancy between measured and computed pressure coefficients is particularly high at specific locations in the TPU wind-tunnel cases. At the

same time, the symmetry of pressure coefficients at building sides (abscissas from 5 to 6 and from 7 to 4) is not systematic. One of the measurement points for the high-rise building is even out of range, the reason for which will be examined in more detail in the next section. This suggests that the uncertainty associated with the peak values for the wind-tunnel TPU measurements might be very high. Unfortunately, the experimental uncertainties are not provided in the TPU database and cannot be estimated without extra information. It is important to note that such behavior is not observed in the Silsoe full scale experiment, for which the expected symmetry is visible in all measurements.

Very good agreement between simulated and measured pressure coefficients, for both mean and standard deviation, were obtained in a recent study for a low-rise building with eaves (Ricci et al., 2017). However, the method employed involved explicit roughness elements and implementation of the MDSRFG synthesizer, which, while very relevant for benchmarking, would not be appropriate for industrial applications due to the long setup and computational times, as discussed below.

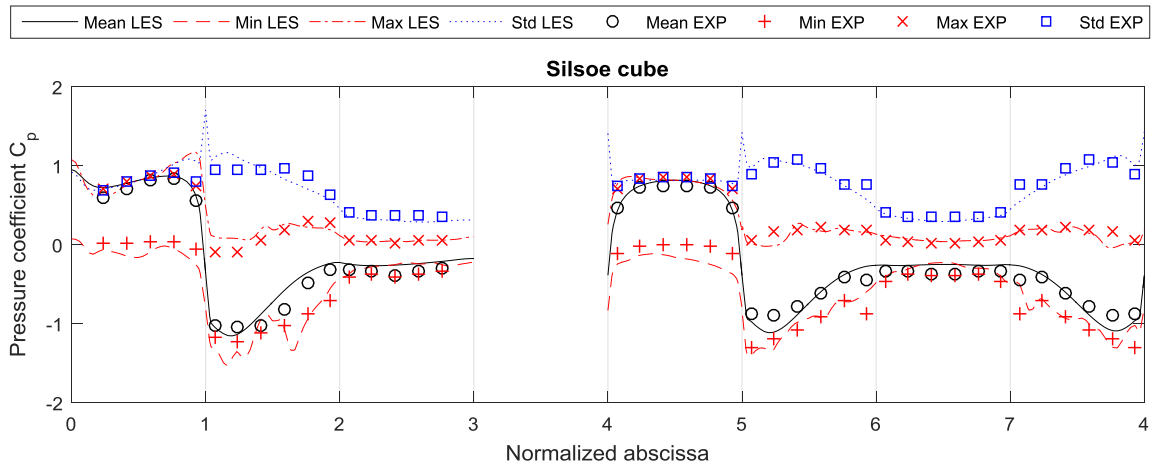

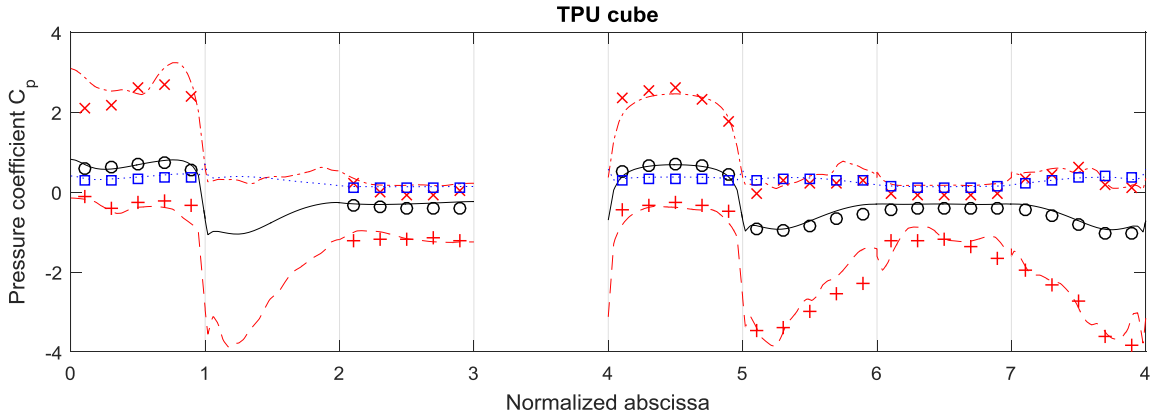

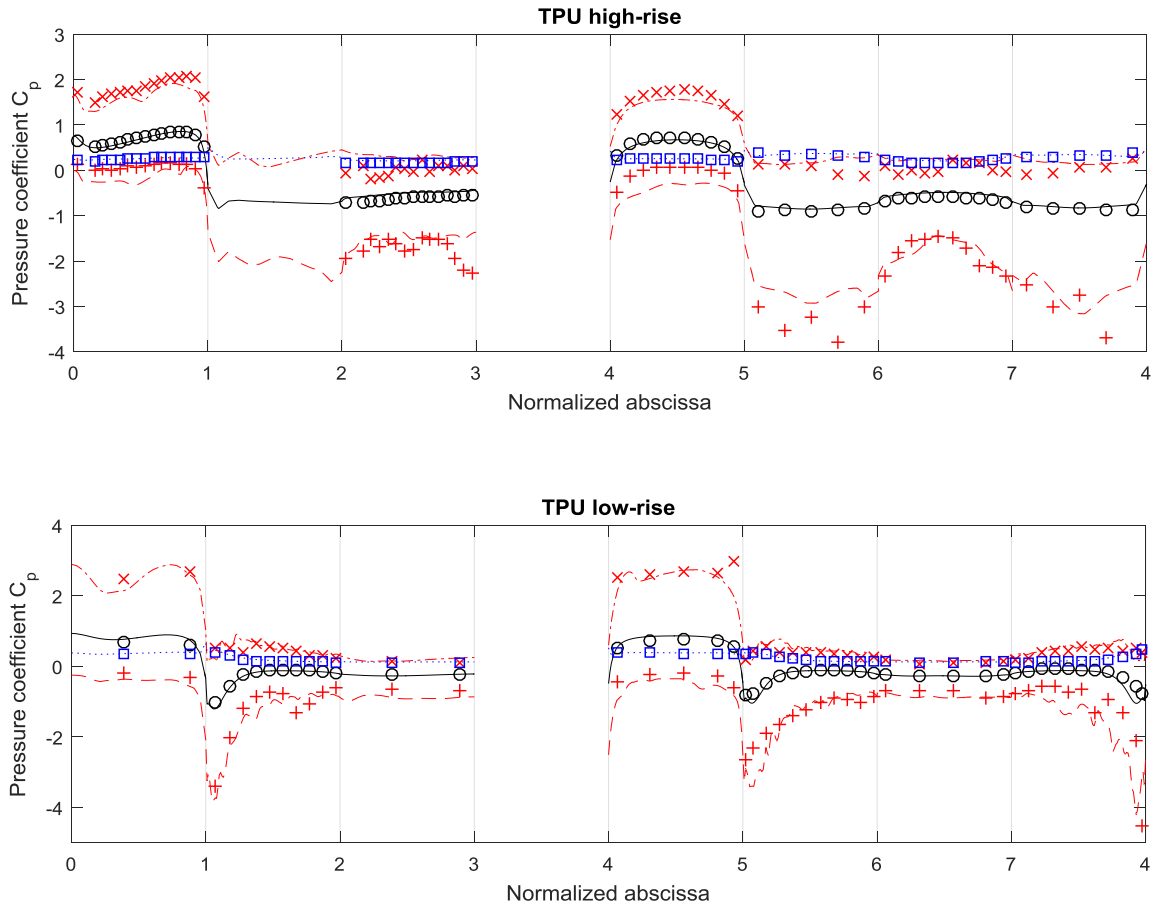

Figure 8 Simulation (Lines, LES) and experimental (Symbols, EXP) pressure coefficients for various shapes of isolated building

5.3 Pressure time series and spectra

In order to identify why the statistics of simulated pressure coefficients differ from experimental data, pressure time series were plotted for two particular locations (Figure 9). These time series are only available for the TPU cases.

The first location (point A) is on the high-rise building, where a vortex is produced from interactions between the airflow and the obstacle. This leads to the highest fluctuations in wind pressure, as seen in Figure 8 near abscissas 5 and 4. This is also the location where discrepancies between simulation and experiment were greatest.

An equivalent location was also retained on the cube (point B) for comparison, as a good agreement between simulation and experiment was obtained here, despite remaining the location where pressure fluctuations were highest.

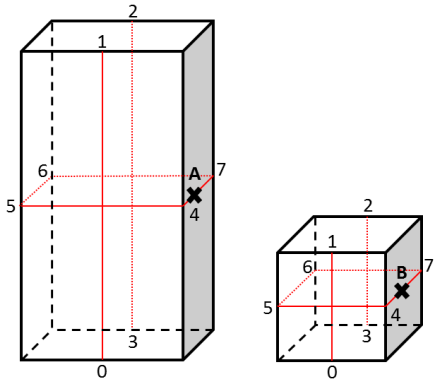

Figure 9 Locations of points A and B used for monitoring pressure coefficients

In Figure 10, time series of pressure coefficients from simulations and experiments are plotted for points A and B over a 32.768 s period. It is clear that the mean, maximum and standard deviation of the pressure are well predicted by the simulation. However, the minimum values differ due to a single negative peak in the experiment at point A. This anomalous peak is likely an experimental artifact since it occurs only once over the period of measurements. Thus, if another run had been carried out, different results might have been obtained. This would support our earlier suggestion that high uncertainties might be associated with the TPU wind-tunnel measurement peak values. Such behavior is not observed at point B, where peak values are reached at least twice over the measurement period, as they are in simulations, making these results more reliable.

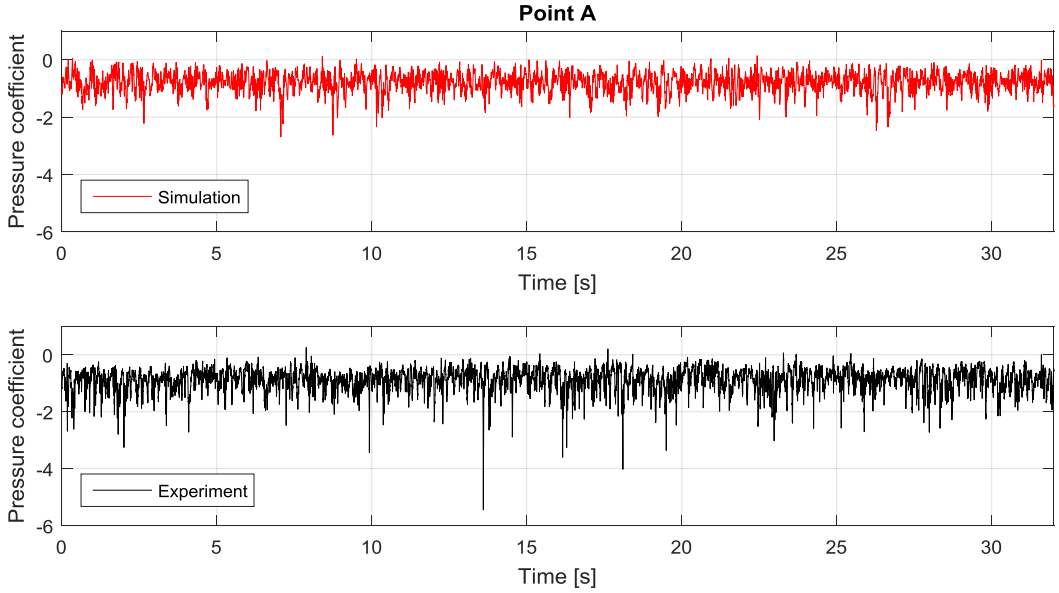

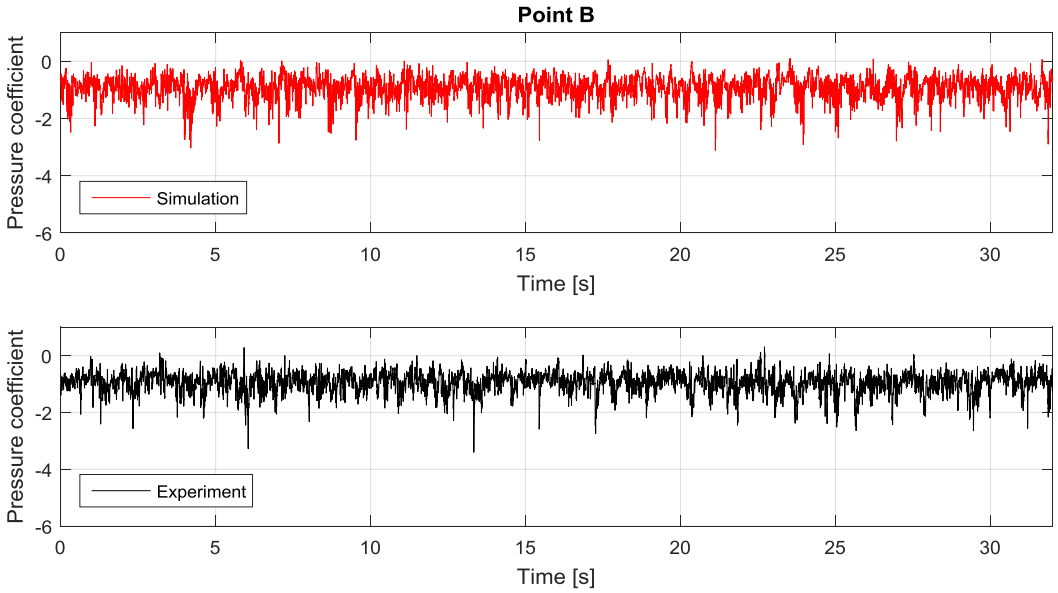

Figure 10 Measured and calculated time series of pressure coefficients at two selected locations, A and B

As experimental data and simulation results have different sampling frequencies, a quantitative comparison can be made by superimposing pressure power spectra, as shown in Figure 11 for points A and B from 0.1 to 500 Hz. This comparison reinforces the observation that the magnitude of pressure is well represented by Large-Eddy Simulation at lower frequencies. However, the comparison also highlights abnormal representations of some high frequencies in the wind-tunnel test at point A, which occur at 228 Hz and 456 Hz, with lower peaks at 114 Hz and 342 Hz. As these frequencies are exact multiples of 114 Hz, they appear to be related to a measurement issue rather than being a real characteristic of the wind turbulence. Once again, no singular frequency is observed in Figure 11 for the experimental pressure power spectrum at point B.

Finally, the particular locations where the deviations between experiment and simulation were highest appear to correspond to those locations where the experimental data raised questions about the consistency of minimum values.

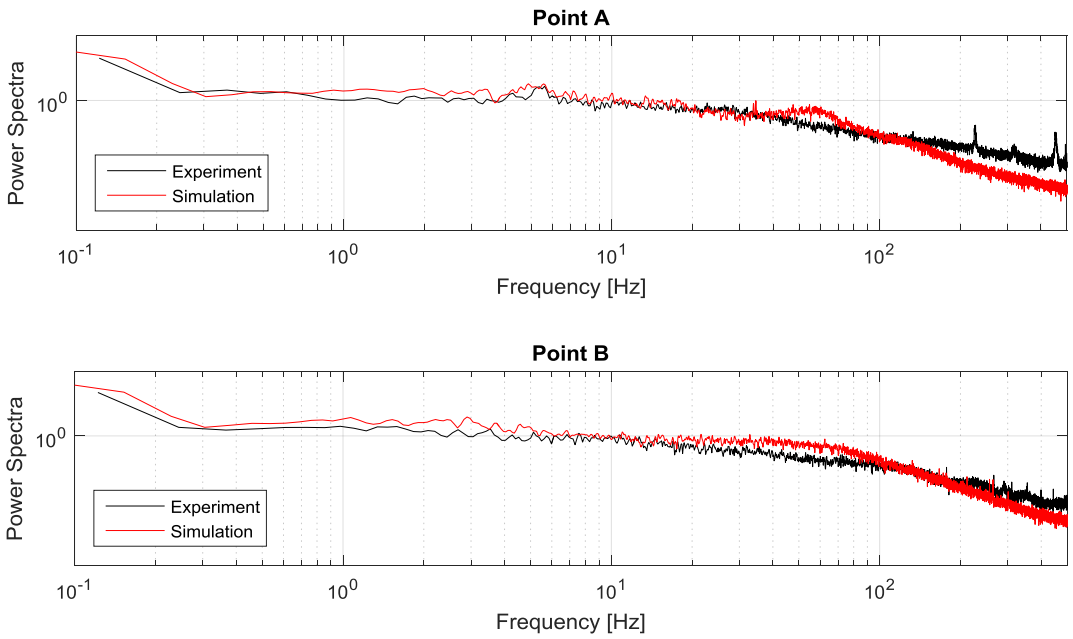

Figure 11 Measured and computed power spectra of pressure coefficients at two selected locations A and B

5.4 Computational cost

The performance of the proposed approach is now assessed for various cases in terms of accuracy, by comparison with reference full scale and wind-tunnel experiments. A major advantage of the method proposed here is claimed to be the significant reduction in both setup and computational times compared to existing approaches.

The setup time is minimized by the use of the automatic cut-cell meshing method (about one million cells) and the Spectral Synthesizer RFG method, a method that has already been implemented and verified in commercial codes.

The computational wall-clock time of one simulation was consistently under 10 hours, covering both initialization and statistical runs, which corresponds to about 1200 CPU hours on the INRS cluster using 128 CPUs (8 nodes, 2 eight-cores Intel Xeon@1.7 GHz and 64 GB RAM per node). This represents 4 times fewer CPU hours than the Silsoe case of Richards and Norris (2015), 20 times fewer CPU hours than the low-rise building case of Ricci et al. (2017), and 4 times fewer CPU hours than the high-rise building case of Yu et al. (2018), without taking into account the fact that the frequencies of the cores used at INRS are always lower than cores used in other studies.

6. Conclusions

Most recent LES studies aimed at predicting unsteady wind pressures on a building have sought to obtain streamwise flow homogeneity, which is particularly relevant in terms of fundamental research. However, it is often difficult to directly apply these recent findings to wind engineering problems because of the high computational costs involved and the time-consuming implementation requirements. The strategy proposed here consists of putting aside the quest for homogeneity and focusing instead on finding a more efficient way to attain targeted flow conditions at the building location.

The method proposed is based on the use of an existing and standard RFG method to produce a divergence-free velocity field at the domain inlet. The inlet turbulence intensity profile must be adapted once using an explicit equation in order to obtain the desired local wind characteristics. The approach was inspired by wind-tunnel experiments in which the flow is first verified without the building and the building is then added to run the final tests.

The main findings of our assessment in the context of wind engineering and industrial applications are as follows:

1. Even though the RFG method produces a Gaussian spectrum at the inlet, it naturally evolves along the domain towards a more realistic spectrum.
2. When the characteristics of the simulated wind are representative of the real flow at the building location, it is possible to obtain an accurate prediction of unsteady wind pressures acting on an isolated building.
3. For wind engineering applications, it seems more cost-effective to aim at achieving realistic wind characteristics at the building location rather than streamwise homogeneity throughout the whole simulation domain.
4. Compared to existing methods (recycling, precursor-successor, iterative methods and other synthetic turbulence generators), the proposed approach involves a lower computational cost and needs no additional developments under commercial codes, making it possible for engineers to apply it immediately.

Next steps will consist of extending the evaluation of the approach to more complex shapes of buildings and to non-isolated buildings, and then using the results to design industrial ventilation systems that are subjected to wind.

References

Aboshosha, H., Elshaer, A., Bitsuamlak, G.T., Damatty, A.E. (2015). Consistent inflow turbulence generator for LES evaluation of wind-induced responses for tall buildings, J. Wind Eng. Ind. Aerodyn. 142, 198–216.

Blocken, B. (2015). Computational Fluid Dynamics for urban physics: Importance, scales, possibilities, limitations and ten tips and tricks towards accurate and reliable simulations, Build. Environ. 91, 219–245.

Castro, H.G., Paz, R.R. (2013). A time and space correlated turbulence synthesis method for Large Eddy Simulations, J. Comp. Phys. 235, 742–763.

Counihan, J. (1975). Adiabatic atmospheric boundary layers: A review and analysis of data from the period 1880-1972, Atm. Environ. 79, 871–905.

Franke, J., Hellsten, A., Schlünzen, H., Carissimo, B. (2010). The best practice guideline for the CFD simulation of flows in the Urban Environment: an outcome of COST 732, Proc. for the 5th International Symposium on Computational Wind Engineering.

Guichard, R. (2017). Large Eddy Simulation of Pressure Fluctuations on a Surface-Mounted Cube, Proc. for the 7th European-African Conference on Wind Engineering.

Huang, S.H., Li, Q.S., Wu, J.R. (2010). A general inflow turbulence generator for large eddy simulation, J. Wind Eng. Ind. Aerodyn. 98, 600–617.

Iousef, S., Montazeri, H., Blocken, B., van Wesemael, P.J.V. (2017). On the use of nonconformal grids for economic LES of wind flow and convective heat transfer for a wall-mounted cube, Build. Environ. 119, 44–61.

Irtaza, H., Beale, R.G., Godley, M.H.R., Jameel, A. (2013). Comparison of wind pressure measurements on Silsoe experimental building from full-scale observation, wind-tunnel experiments and various CFD techniques. Int. J. Eng. Sci. Technol. 5, 28–41.

Köse, D.A., Dick, E. (2010). Prediction of the pressure distribution on a cubical building with implicit LES, J. Wind Eng. Ind. Aerodyn. 98, 628–649.

Kraichnan, R.H. (1970). Diffusion by a random velocity field, Phys. of Fluids 13, 22–31.

462 Lamberti, G., Garcia-Sanchez, C., Sousa, J., Gorlé, C. (2018). Optimizing turbulent inflow
463 conditions for large-eddy simulations of the atmospheric boundary layer, J. Wind Eng. Ind.
464 Aerodyn. 177, 32–44.

465 Le Roux, N., Faure, X., Inard, C., Soares, S., Ricciardi, L. (2013). Reduced-scale study of
466 transient flows inside mechanically ventilated buildings subjected to wind internal
467 overpressure effects, Build. Environ. 62, 8–32.

468 Nicoud, F., Ducros, F. (1999). Subgrid-scale stress modelling based on the square of the
469 velocity gradient tensor, Flow Turbul. Combust. 62, 183–2000.

470 Oke, T. (1987). Boundary Layer Climates. London: Routledge.

471 Papadopoulos, A., Guichard, R., Van Hoof, T., Fontaine, J.R., Blocken, B. (2018).
472 Measurements of Wind Effects on the Efficacy of Asbestos Containment in a High-Rise
473 Building, Proc. for the Roomvent & Ventilation Conference.

474 Poletto, R., Craft, T., Revell, A. (2013). A New Divergence Free Synthetic Eddy Method for
475 the Reproduction of Inlet Flow Conditions for LES, Flow Turbul. Combust. 91, 519–539.

476 Ricci, M., Patruno, L., De Miranda, S. (2017). Wind loads and structural response:
477 Benchmarking LES on a low-rise building, Eng. Struct. 144, 26–42.

478 Richards, P.J., Hoxey, R.P. (2012). Pressures on a cubic building, Part 1: Full-scale results. J.
479 Wind Eng. Ind. Aerodyn. 102, 72–86.

480 Richards, P.J., Hoxey, R.P., Connell, B.D., Lander, D.P. (2007). Wind-tunnel modelling of
481 Silsoe Cube, J. Wind Eng. Ind. Aerodyn. 95, 1384–1399.

482 Richards, P., Norris, S. (2015). LES modelling of unsteady flow around the Silsoe cube, J.
483 Wind Eng. Ind. Aerodyn. 144, 70–78.

484 Smirnov, A., Shi, S., Celik, I. (2001). Random flow generation technique for large eddy
485 simula-tions and particle-dynamics modeling, J. Fluids Eng. 123, 359–371.

486 Tominaga, Y. et al. (2008). AIJ guidelines for practical applications of CFD to pedestrian
487 wind environment around buildings, J. Wind Eng. Ind. Aerodyn. 96, 1749–1761.

Vasaturo, R., Kalkman, I., Blocken, B., van Wesemael, P.J.V. (2018). Large eddy simulation of the neutral atmospheric boundary layer: performance evaluation of three inflow methods for terrains with different roughness, J. Wind Eng. Ind. Aerodyn. 173, 241–261.

Xie, Z.T., Castro, I.P. (2008). Efficient Generation of Inflow Conditions for Large Eddy Simulation of Street-Scale Flows, Flow Turbul. Combust. 81, 449–470.

Yan, B.W., Li, Q.S. (2015). Inflow turbulence generation methods with large eddy simulation for wind effects on tall buildings, Comp. & Fluids 116, 158–175.

Yu, Y., Yang, Y., Xie, Z. (2018). A new inflow turbulence generator for large eddy simulation evaluation of wind effects on a standard high-rise building, Build. Environ. 138, 300–313.